

REFRACTION AND TOTAL REFLECTION OF MICROWAVES BY A PRISM

REFRACTION, TOTAL REFLECTION, AND DIFFRACTION  
OF  
3.2 CM. ELECTROMAGNETIC WAVES BY A DIELECTRIC PRISM

By

DAVID RANDOLPH KNEELAND, B.Sc.

A Thesis

Submitted to the Faculty of Arts and Science  
in Partial Fulfilment of the Requirements  
for the Degree  
Master of Science

McMaster University

October, 1954

MASTER OF SCIENCE (1954)  
(Physics)

McMASTER UNIVERSITY  
Hamilton, Ontario

TITLE: Refraction, Total Reflection, and Diffraction of 3.2 cm.

Electromagnetic Waves by a Dielectric Prism

AUTHOR: David Randolph Kneeland, B.Sc. (McMaster University)

SUPERVISOR: Professor A. B. McLay

NUMBER OF PAGES: 20, (with 7 figures)

SCOPE AND CONTENTS:

A description of several experiments carried out to investigate the behaviour of 3.2 cm. microwaves on passing through a dielectric prism is given in this thesis. Chapter I contains a description of the experimental apparatus used to generate electromagnetic radiation and to measure the field intensity in a plane perpendicular to the refracting edge of the prism. Particular emphasis is placed on a description of the receiver amplifier, and on the construction of the wax prism.

In Chapter II are given the results of several preliminary investigations of the field close to, and polarized parallel to the refracting edge of the prism. Fresnel interference fringes were observed with the prism oriented as a biprism. Diffraction fringes of a  $45^\circ$  wedge, both dielectric and metallic, were observed incidentally. Evidence of the evanescent wave predicted for total internal reflection was obtained directly in this experiment where earlier evidence of such waves in the optical and microwave regions has been indirect.

### ACKNOWLEDGEMENTS

The author wishes to express his gratitude to Professor A. B. McLay for his constant encouragement and guidance during the course of this project. The many helpful discussions of the theoretical aspects with Dr. M. A. Preston are very much appreciated.

Thanks are due also to Mr. M. K. Subbarao for his assistance in setting up the experimental apparatus, and to Mr. S. T. Wiles, who gave freely of his time for consultation regarding the operation of the microwave transmitter.

The Imperial Oil Company kindly supplied the special paraffin wax which was used to construct the prism.

The author wishes to thank the Research Council of Ontario for personal financial assistance in the form of a scholarship.

The project has received financial aid from the generous support of the National Research Council of Canada.

## TABLE OF CONTENTS

	page
INTRODUCTION . . . . .	1
CHAPTER I	
EXPERIMENTAL APPARATUS	
(i) The Transmitter . . . . .	3
(ii) The Probe and Track . . . . .	3
(iii) The Amplifier and Recorder . . . . .	4
(iv) The Dielectric Prism . . . . .	6
CHAPTER II	
EXPERIMENTAL PROCEDURE AND RESULTS	
(i) Experimental Procedure . . . . .	8
(ii) Microwave Interference Fringes Behind a Biprism . . . . .	9
(iii) The Totally Reflecting Biprism . . . . .	11
(iv) The Single Totally Reflecting Prism . . . . .	13
(v) The Lateral Shift of the Reflected Ray . . . . .	14
APPENDIX . . . . .	16
REFERENCES . . . . .	20

LIST OF DIAGRAMS

- Figure 1    Narrow Band Amplifier
- 2    Experimental Interference and Diffraction Fringes Behind the Biprism
- 3    Diffraction Fringes of  $45^\circ$  Conducting Wedges
- 4    Diffraction Fringes of  $45^\circ$  Dielectric Wedge and Evanescent Wave at a Totally Reflecting Surface
- 5    Interference Fringes of the Evanescent Wave Behind the Prism
- 6    The Field Behind the Single Reflecting Prism
- 7    Evanescent Wave Near the Surface of the Totally Reflecting Prism

## INTRODUCTION

In recent years, workers in the field of optics have been studying a peculiar phenomenon associated with the total reflection of an electromagnetic wave from the boundary surface of two dielectric substances. Maxwell's laws, and the Fresnel equations predict the existence of a wave motion in the less dense medium close to the interface of the more dense dielectric. This excitation is a nontransverse wave travelling parallel to the surface, and decreasing exponentially to a very small intensity within a few wavelengths of the face.

Evidence of the existence of this evanescent wave has been detected in several ways. Wood (13) placed small particles of soot on the totally reflecting surface of a glass prism and observed under a microscope that the particles emitted scattered light from all sides. Bruhat (3) describes an experiment wherein the totally reflecting faces of two prisms are placed together, one of the prisms having a slightly convex reflecting face. At the point of optical contact, white light is transmitted and appears as a white spot surrounded by a red ring, while the reflected light shows a dark spot surrounded by a blue ring. The red light, being of larger wavelength, is able to penetrate the small air gap close to the point of contact as an evanescent wave, and enter the second prism where it reverts to a transverse wave form. Hall, Wood and others, using this apparatus with monochromatic light have observed Newton's rings in the reflected beam, and a complementary pattern in the transmitted beam. Some of the incident light penetrates the boundary of the first surface far enough

to be appreciably reflected from the second one, and air-to-glass phase changes result in the interference pattern.

An examination of the equations of the reflected light (appendix) will show that there is a phase difference between the two polarization components upon total reflection. Culshaw (4) was able to change this phase difference, using microwave radiation, by placing a conducting plate in the evanescent wave region of a totally reflecting prism, thus giving evidence of its existence.

One effect of the penetration of the second medium at total reflection is to laterally displace the reflected ray in the direction of propagation of the incident beam. Goos and Hanchen (6) describe a method for detecting this displacement. In the experiment, multiple reflections of a beam of light occur, part of the beam falling on a silvered mirror, and part on a glass air interface. As many as 74 such reflections take place, rendering the relative lateral displacement of the two parts of the beam subject to accurate measurement.

This and other indirect optical effects have offered proof of the existence of this disturbance, but direct observation of the evanescent wave has not been practicable with visible light because of the extremely short wavelengths.

At the suggestion of Professor A. B. McLay, the author has carried out several experiments to detect the evanescent waves emerging from the face of a totally reflecting dielectric prism using 3.2 cm. electromagnetic radiation. These are described in this thesis, as well as a study of the interference fringes produced by a Fresnel biprism. The diffraction fringes of a  $45^\circ$  dielectric wedge and conducting wedge were observed incidentally.



(i) The Transmitter

A 723 A/B reflex klystron oscillator, with a TVN-7BL power supply and modulator, was used to generate 9375 Mc/s oscillations. (8) (12) These were reflector modulated by an 800 c/s square wave, this modulation frequency being chosen to match the single frequency response of the receiver amplifier. The 3.2 cm. waves were radiated by a 23° E - H pyramidal aluminium horn measuring 73.5 cm. long, with a 31 by 30 cm. aperture. This horn, built by Keys, (7) was designed to concentrate the beam in the horizontal and vertical planes to reduce possible reflections from the walls, and the ceiling and floor of the laboratory, and in the experiments described in this thesis, was mounted so as to polarize the electric field vector in a vertical plane.

A directional coupler, inserted between the klystron and horn, fed a cavity absorption wavemeter, which was used to set the frequency. Fluctuations of the amplitude and frequency of the klystron oscillations caused by draughts on the room were reduced by utilizing a blower to cool the klystron. The steady air stream passing directly over the walls of the tube protected it from random air currents and resulted in a steadier output. After a suitable warming-up period, the frequency was found to vary less than 1 part in 10,000.

(ii) The Probe and Track

A 1N23A crystal diode was used as a probe to measure field intensities directly, considering it to be a square-law detector. The metal

ends of the cartridge were turned down to 1 mm. rods, forming a simple dipole antenna. This was mounted at the wedge-shaped end of a hard rubber tube, in the same manner as used by Wiles (12) and Keys (7). The probe assembly was carried by a wooden stand fitted onto an optical bench base. A lead screw, driven by a 1/8 h.p. synchronous motor and 1:100 reducing gear, served to drive the base along an optical bench, permitting the probe to be moved along any desired line in the X - Y plane of the system.

### (iii) The Amplifier and Recorder

The 800 c/s. square wave signal detected by the probe was led through the hard rubber tube to the wooden stand, then down to the floor and along to the amplifier, which was mounted in an instrument rack along with the transmitter and recorder. The output of this amplifier was rectified and fed to a Brown Electronik Potentiometer, giving a continuous record of field intensity at the probe position. The unit used earlier by Wiles and Keys was a broad band a-c amplifier with a maximum gain of 35,000, with output clamped by a diode, and a small part fed to the recorder. It used a variable gain setting. At the beginning of the present project this amplifier became unstable and difficult to adjust due to the ageing of components. It has been redesigned and rebuilt by M. K. Subbarao and the author, but a new unit designed and built to replace it was finally used. This latter was a narrow band amplifier permanently adjusted to reject all but 800 c/s. signals, thus eliminating much of the noise and parasitic oscillation of the original unit. A vacuum tube voltmeter was used in the final stage to simplify control of the recorder, and adjust the linearity of the system.

A schematic diagram of the narrow band amplifier is shown in Fig 1. The first stage is a high gain r-c coupled pentode amplifier, the crystal

feeding directly to the control grid in parallel with a 2 megohm resistor. The second stage includes a potentiometer in the input, controlling the gain of the amplifier, and is shunted by the "Twin T" filter network. This filter offers a low impedance path to all frequencies except the resonant frequency of 800 c/s. In this way, all the nonresonant signals are fed back to the input of the stage in inverse phase, and are cancelled out, while the desired signal is amplified and passed through to the third amplifying stage. This third stage is similar to the first. Decoupling condensers and resistors are provided in the plate circuits of each stage to prevent oscillation. Overall gain was not measured accurately, but was estimated to be greater than 50,000. The amplifier has been found to be very stable, and non-microphonic in spite of the high gain.

The 6AL5 diode serves as a negative clamping circuit to provide the direct current required by the recorder. The d-c pulse signal is fed to one triode of the 12AU7 which acts as a cathode follower vacuum tube voltmeter. The amplitude of this signal is varied by the 0.5 megohm potentiometer in the cathode follower grid circuit. This governs the amplitude of the trace on the recorder, and is normally fixed during a series of runs. The recorder, shunted by a 200 ohm matching resistor is tapped into the cathode load of the 12AU7. The position of this tap governs the linearity of the output stage, and thus of the whole amplifier. It was found necessary to ground one side of the recorder to eliminate random variations of the zero line, and this necessitated the use of a separate plate supply for the output stage. A 90 volt battery was used, in parallel with a one megohm potentiometer. The tap on this potentiometer varies the level of the plate above ground, and controls the zero signal level of the recorder in doing so.

The amplifier was powered by a Hewlett-Packard Model 710A regulated power supply. Line voltage variations were reduced by employing a Sola constant voltage transformer in the power line to all equipment except the drive motor for in the probe mechanism.

(iv) The Dielectric Prism

Paraffin wax is a low loss dielectric substance with a refractive index sufficiently high to ensure total internal reflection for an incident angle of  $45^\circ$ . This feature, along with its low melting point and low cost made it the logical choice of material for the fabrication of the prism.

A mold was assembled of  $3/4$ " plywood sheets bolted together to form a  $90^\circ$  V shaped trough, 18" long, and 13" deep, with closed ends, the 18" sides being set at  $45^\circ$  to the horizontal. The inside was lined with heavy aluminium foil to prevent adhesion of the wax to the plywood, and the mold was shimmed to level the top edges. A large double boiler served to melt the 90 lbs. of paraffin required, and the molten wax was transferred to the mold by means of a polythene siphon tube to minimize air entrainment. As the wax solidified, it contracted to form a hollow in the upper surface. Electric heaters in photoflood lamp reflectors were used to heat the upper surface and more molten wax was added to fill the indentation. Thereafter, alternate heating and cooling of the upper face allowed it to form a sufficiently flat surface. Upon removal from the mold, the faces were scraped to remove several small indentations caused by wrinkles in the aluminium lining, and to improve the corners. The prism used in the final experiments was found to measure 44.2 cm. by 43.7 cm., by 61.5 cm., and stood 45.7 cm. high.

Two grades of paraffin wax were tried. The first was a standard

product of the Imperial Oil Company, normally used to wax papers and turnips, with a melting point ranging from 133°F to 136°F. It was found that bubbles appeared in this wax during solidification. These bubbles could be seen below the surface, distributed throughout the prism in a random manner, and ranging in diameter from 1/16" to 1/4". It was thought that these bubbles would scatter the radiation, masking the diffraction and interference fringes, and attempts were made to eliminate them. Consultation with Imperial Oil Company revealed, however, that the bubbles were due to the release of dissolved air in the molten wax as it solidified, and were virtually impossible to eliminate. The company then provided a special wax with an oil additive, having a melting point of 157°F. Another prism was cast of this wax and showed no bubbles, but rather a crystallization with a similar distribution. Lack of time prevented further investigation, and this second prism was used in the experiments. If scattering occurred, it did not mask the patterns, but may have been partly responsible for some of the irregularities encountered.

The prism was mounted at the level of the microwave beam on 8" high polystyrene foam blocks, a substance transparent to microwave radiation. The blocks were set on a plywood box resting on a wheeled table. The prism was then easily moved to any desired position and orientation.

Parasitic reflections in the laboratory were reduced by placing sheets of absorbing material in front of them. This material is formed of animal fiber coated with a mixture of conducting carbon black in neoprene to form a lossy material. This Microwave Absorbing Material was obtained from the Sponge Rubber Products Company of Shelton, Connecticut, U. S. A., in the form of 2' by 2' by 1 1/2" sheets. The material reflects less than 2% of the radiation incident upon it, and has proven very effective in the above application.

(1) Experimental Procedure

For the field measurements, the transmitter was mounted at one end of a room measuring 25' wide and 75' long. The horn was elevated to a position midway between the floor and ceiling and equidistant from the two side walls, and oriented to propagate vertically polarized radiation down the long axis of the room. The probe and track were located 8 meters from the apex of the horn along the axis of propagation, termed the x axis, and set to move along a horizontal line perpendicular to it, the y axis.

Reflections and scattering from certain vertical water pipes and metal panels at the side walls and from the far end of the room, although not too pronounced, were located and reduced by screening them with sheets of the absorbing material. Runs made of the open field showed that the amplitude of the incident radiation was fairly uniform over 80 cm., except for small irregularities which could not be eliminated. It was felt that these were caused partly by slight imperfections in the horn radiator.

The prism was mounted with its refracting edges vertical and their midpoints in the horizontal plane of propagation of the horn (x - y plane). After location of the prism in its chosen position for each experiment, the probe was moved along the x axis to selected distances from a convenient face of the prism by sliding the probe forward or backward in the wooden upright. Calibration of the motion in the y direction was effected by starting the recorder as the carriage moved past a mark on the optical bench, and by stopping at a similar mark at the end of the run. The positive y direction was chosen to extend to the right of the axis of propagation,

looking toward the source.

(ii) Microwave Interference Fringes Behind a Biprism

A Fresnel biprism (9) was formed by locating the prism symmetrically about the x axis, with the  $90^\circ$  apex pointing toward the source. The hypotenuse face was thus perpendicular to the axis of propagation, and its midpoint was taken as the origin. The probe was run parallel to this face over an 80 cm. range to include the effect beyond the prism corners, at distances from 0.8 cm. to 75 cm. away from the face.

The resulting patterns, plotted in Fig. 2, show the Fresnel interference fringes in a diamond shaped region where the refracted beams from the two halves of the prism overlap one another. It was noted that the fringe spacing was not constant, but decreased from a maximum of 4 cm. near the face close to the x axis to a minimum of 3 cm. at the edges of the interference region. The spacing also decreased, though not so noticeably, further back from the face, the average separation falling from 3.85 cm. close to the face to 3.75 cm. 14 wavelengths to the rear. In the optical case, the fringe width is constant along a line normal to the direction of propagation, and increases further from the prism. The difference is due to the distance from the prism to the point of observation, relative to the distance from the source to the prism, the ratio being very large in the normal optical case, and small in the present experiment. In the optical case also the refracting angle of the biprism is much less than here, with the result that the interference region extends to infinity rather than forming a diamond shaped region.

The microwave interference peaks are typical of those found in optics in that they range from two to four times the intensity of the incident field.

This feature distinguishes them from the remaining intensity variations beyond the edges of the prism, and within the geometrical shadow but outside the interference region. These latter are due to diffraction effects of the apex and corners of the prism. The diffraction fringes of the  $45^\circ$  dielectric wedge corners are particularly interesting as the author is not aware of any previous studies on such effects. A more complete investigation of this case would be desirable, but is beyond the scope of the present work, and is left to future workers.

The geometrical path of the radiation passing through the prism, outlined by the dashed lines in Fig. 2 is not claimed to be exact. The lines were obtained by employing a best fit method to determine the edges of the interference region, and adjusting to satisfy Snell's law of refraction. An approximate value of 1.58 for the refractive index of the prism was obtained in this way, and insured total internal reflection for an angle of incidence greater than  $39^\circ$  in the later experiments.

In order to determine the effect of radiation coming around the prism from the corners, or the top and bottom surfaces, a set of runs were made with the refracting faces coated with aluminium foil to prevent transmission. The results in Fig. 2 show that there is no radiation in the shadow of the prism as far back as 28 cm., and runs not shown indicated a negligible field intensity out to 75 cm. from the face. A sharply defined diffraction pattern of the  $45^\circ$  conducting wedge was observed 0.8 cm. from the face extending outward from each corner of the prism. The fringes appear to spread in width and separation further back from the corner. These effects are typical of those observed by Row (10) for metallic wedges, although in his work, the wedge was mounted with the incident face normal



to the direction of propagation.

(iii) The Totally Reflecting Biprism

Following the biprism experiment, the prism was rotated through an angle of  $180^\circ$  so that the incident radiation fell normally upon the hypotenuse face, with the apex pointing in the direction of propagation. A lateral translation brought the right hand edge of the prism to the centre of the beam, and this corner was taken as the  $x - y$  origin of the co-ordinate system. The probe was run parallel to the incident face from points as close as possible to the  $45^\circ$  face out to the right hand edge of the field. Runs were made at intervals of one wave length from the projection of the incident face, but only half of these are shown in Fig. 4 to avoid crowding in the diagram.

The radiation entering the prism strikes the rear faces at a incident angle of  $45^\circ$  and is totally reflected. Travelling across the prism, it falls upon the opposite face and is again totally reflected and proceeds back along the axis of propagation toward the source. The beams from each half of the incident face interfere and set up standing waves inside the prism.

The resulting intensity variations in Fig. 4 show evidence of a diffraction pattern extending to the right of the  $45^\circ$  corner, and filling the field to the right of the geometric shadow edge.

The fact that the fringe spacing remains constant, and of the order of one wavelength throughout the region, rather than spreading, as in the normal wedge diffraction pattern seen in Fig. 2, indicates the presence of radiation interfering with the incident field, and superimposing an interference pattern on the typical diffraction fringes. This may result from a diffraction effect of the small relative aperture of the incident and

reflecting faces. Diffraction of the beam incident upon the totally reflecting face on the left side of the prism (looking into the source) could permit some of the radiation to strike the right hand face within the critical angle. This radiation, escaping from the prism, would proceed across the diffraction region, interfering with the incident radiation, and result in the observed pattern.

It is seen that the field in the geometric shadow of the prism falls to a very low intensity except close to the reflecting face. The strong field in this region is taken to be an evanescent wave emerging from the totally reflecting surface, as predicted by electromagnetic theory. Although there is a possibility that this disturbance could be due to radiation striking the reflecting face at less than the critical angle of incidence and emerging into the less dense medium, further evidence to be shown supports the assumption that the field is due to an evanescent wave, and it will be taken and referred to as such in this thesis.

The intensity can be seen to fall off rapidly a short distance from the face. This is in agreement with the predicted exponential decrease of the evanescent field in a direction normal to the surface, wherein the intensity drops to a negligible level within a few wavelengths.

The variation of the evanescent field intensity, parallel, and as close as could be detected, to the surface might be accounted for by considering the effect of the two reflected beams in the prism, which set up evanescent waves travelling in opposite directions along the boundary to create a standing wave pattern.

A definite interference pattern of two evanescent waves, one from each reflecting surface appears in the region directly behind the apex of the prism. Fig. 5 shows the resulting intensity variations caused by the inter-

action of these waves travelling along the surfaces toward the apex. It can be seen that the field diminished in both the x and the y directions, falling to a very low value within two wavelengths of the apex. One interesting feature noted is that the centre peak rises to a maximum a short distance from the apex before drying out. This was more evident in the complete set of patterns, of which only three are shown for simplicity. The asymmetry of the right and left sides of the pattern is probably due to a combination of the inhomogeneity of the prism and a lack of perfect geometry within the system.

#### (iv) The Single Totally Reflecting Prism

To avoid the complications of interfering wave motions found with the totally reflecting biprism, the prism was located so as to singly reflect the incident beam through  $90^\circ$ . The arrangement is shown in Fig. 6, with the hypotenuse face serving as the totally reflecting boundary, and the two smaller faces as the incident and emergent surfaces. Radiation incident on the hypotenuse face at  $45^\circ$  was reflected to the left, or in the negative y direction. The probe was run as before parallel to the incident face, and as close as possible to the totally reflecting surface.

A wedge edge diffraction pattern appeared to the right of the geometrical shadow edge, and extended slightly into the shadow region. The majority of the space behind the prism however was quite dark, indicating that there was no radiation passing through the region from either the corner or the reflecting face, as there was in the biprism case.

Close to the face, the field was again found to be very intense, at some points considerably higher than the incident field level. This is again indicative of an evanescent disturbance, in this case of a single total

reflection and displays the characteristic rapid decrease of intensity away from the face.

The field of this evanescent wave was further investigated by running the probe parallel to the totally reflecting face at several distances from the surface. The results of three runs are shown in Fig. 7, where the y axis has been chosen as a line coincident with the hypotenuse face of the prism, with origin at the mid-point. The decrease of the field intensity out to 3.2 cms. away from the face is clearly indicated in the figure, and a further run at 6.4 cms., not shown, indicated negligible field at that distance.

The rapid and somewhat irregular fluctuation of the field intensity along the face has not been accounted for as yet, and further work is necessary to determine the cause. Diffraction by the aperture of the incident face, which is quite small in terms of wavelengths, is probably responsible for the variations in the envelope of the peaks. A similar pattern was observed in the field of the reflected radiations emerging from the prism.

#### (v) The Lateral Shift of the Reflected Ray

With the prism mounted as in the preceding experiment, an attempt was made to measure the lateral shift suffered by a totally reflected ray in the direction of propagation. The probe was run parallel to the axis of propagation at various distances from the emergent face of the prism, and across the totally reflected beam.

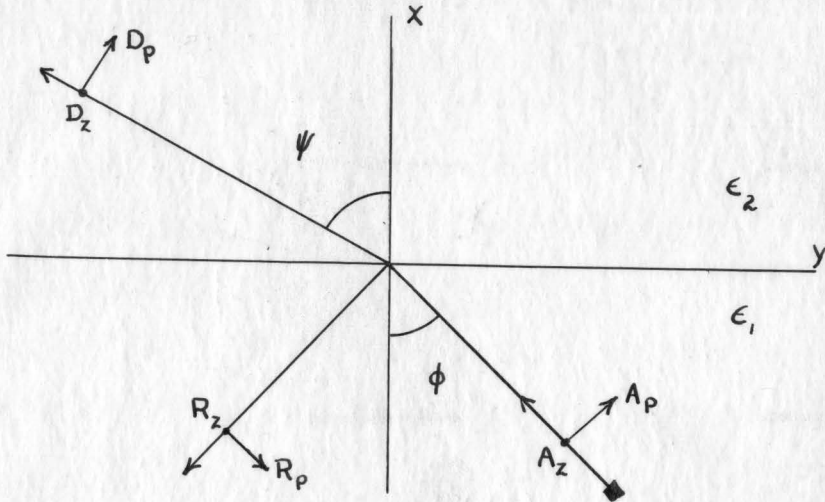
The first runs showed a strong interference pattern in the emerging beam, which was caused by interference of the reflected beam with the incident radiation falling directly into the region. This latter was eliminated by mounting a large conducting plate in line with the incident face, and extending to the right from the corner of the prism. No incident radiation

could then enter the space, and when the incident face of the prism was blocked by absorbing material, no field at all was observed.

Upon removal of the absorber, the beam showed large variations suggestive of the diffraction pattern of an aperture, but the peaks were not symmetrical, making it impossible to locate the centre of the beam.

Strips of metal were next placed over the incident face to form single or double slits. It was hoped that a recognizable diffraction or interference pattern could be formed in the reflected beam, which could be traced geometrically through the prism in order to determine the lateral shift. Single slits varying from 3.2 cm. to 14 cm. in width were tried, but the resulting patterns were too asymmetrical to be of use. Several double slits, ranging in width from 1 cm. to 6.6 cm., and in separation from 9 cm. to 32 cm. did not produce intelligible interference patterns due to a lack of intensity.

Another approach to the problem was to coat the reflection surface with aluminium foil, causing metallic reflection which would not shift the reflected beam because there is no penetration of the conducting medium. Comparison of a beam pattern with and without the metal reflector would show the lateral shift. Each of the aforementioned slit arrangements were studied with and without the metal backing, but unfortunately the patterns were altered to such an extent by the metal that it was impossible to correlate them.

APPENDIXTheory of Total Reflection and the Equations of the Evanescent Wave

Consider a plane electromagnetic wave incident on the boundary of two non-dispersive media of dielectric constants  $\epsilon_1$  and  $\epsilon_2$  where  $\epsilon_1 > \epsilon_2$ . Maxwell's equations yield Snell's law

$$n_{12} = \sqrt{\frac{\epsilon_2}{\epsilon_1}} = \frac{\sin \phi}{\sin \psi}$$

$n_{12}$  = relative refractive index,

$\phi$  = angle of incidence,

$\psi$  = angle of refraction,

and the phase factor of the refracted ray

$$\gamma_D = k_2(c_2 t + y \sin \psi - x \cos \psi) \quad (1)$$

where  $\underline{E} = \underline{D} e^{i\gamma_D}$ ,  $\underline{E}$  = electric field vector (2)

$k_2$  = the wave number in the second medium

$\underline{D}$  = the wave amplitude

The Fresnel equations for the two polarizations of the refracted ray are

$$\frac{D}{P} = \frac{2 \sin \psi \cos \phi}{\sin(\phi + \psi) \cos(\phi - \psi)} \frac{A}{P} \quad (3)$$

$$\frac{D}{Z} = \frac{2 \sin \psi \cos \phi}{\sin(\phi + \psi)} \frac{A}{Z} \quad (4)$$

where  $\frac{D}{P}$ ,  $\frac{A}{P}$ , and  $\frac{D}{Z}$ ,  $\frac{A}{Z}$  refer to polarization in the plane of incidence, and normal to the plane of incidence respectively.

These formulae are valid for all values of  $\epsilon_1$  and  $\epsilon_2$  and all angles of incidence. However, let  $\phi = \phi_0$ , when  $\sin \psi = 1$ , i.e.  $\sin \phi_0 = n_{12}$ .

If  $\phi_0 > \phi > 0$ , then  $\psi$  exists and is real.

If  $\phi > \phi_0$ , the above equations hold only for complex values of  $\psi$ .

$$\text{Writing } \sin \psi = \frac{\sin \phi}{n}, \quad \cos \psi = \pm \frac{i}{n} \sqrt{\sin^2 \phi - n^2} \quad (n = n_{12})$$

where the choice of sign before the radical will be governed by the condition that the field shall never become infinite.

Substitution into equation (4) yields

$$\begin{aligned} \frac{D}{Z} &= \frac{2 \sin \phi \frac{i}{n} \sqrt{\sin^2 \phi - n^2}}{\sin \phi \frac{i}{n} \sqrt{\sin^2 \phi - n^2} + \frac{\cos \phi \sin \phi}{n}} \\ &= \frac{2 \sqrt{\sin^2 \phi - n^2}}{(1 - n^2)^{\frac{1}{2}}} \left[ \frac{\sqrt{\sin^2 \phi - n^2}}{(1 - n^2)^{\frac{1}{2}}} + \frac{i \cos \phi}{(1 - n^2)^{\frac{1}{2}}} \right] \end{aligned}$$

$$= \frac{2}{n} \cos \chi e^{i\chi} \quad \text{where} \quad \chi = \tan^{-1} \frac{\cos \phi}{\sqrt{\sin^2 \phi - n^2}}$$

$$\frac{D_z}{n} = \frac{2}{n} \cos \chi \frac{A_z}{n} e^{i\chi}$$

and from (2)

$$\frac{E_z^D}{n} = \frac{2}{n} \cos \chi \frac{E_z^A}{n} e^{-\frac{k_2}{n} \sqrt{1-n^2} \cos \chi x} e^{ik_2(ct + y \frac{\sin \phi}{n} + \frac{\chi}{k_2})}$$

similarly

$$\frac{E_p^D}{p} = 2 \cos \Omega \frac{E_p^A}{p} e^{-\frac{k_2}{n} \sqrt{1-n^2} \cos \chi x} e^{ik_2(ct + y \frac{\sin \phi}{n} + \frac{\Omega}{k_2})}$$

$$\text{where } \tan \Omega = n^2 \tan \chi.$$

References (2) (11)

The two components of the evanescent wave show that the motion travels in the y direction, and decreases exponentially in intensity away from the boundary in the x direction. The positive sign is chosen before the radical in the expression for  $\cos \psi$ , since the negative sign would predict an intensity increasing in the x direction without limit.

The order of magnitude of the penetration is given by

$$\frac{c_2}{\omega} = \frac{\lambda_2}{2\pi}$$

where  $\lambda_2$ ,  $c_2$ , are the wavelength and velocity in the second medium, and is thus of the order of a wavelength. Such waves with locally variable amplitudes are called "inhomogeneous waves"; they are not transverse, since the component of the electric vector does not vanish.

Although a field exists in the less dense medium, no average flow of energy takes place across the boundary in the steady state. This can be



verified by showing that the normal component of the Poynting vector possesses a vanishing time average, although there is a to and fro oscillation of energy across the surface. It can be further shown that the reflected ray is equal in amplitude to the incident ray, and thus all the incident energy is reflected.

Artmann (1) has calculated the magnitude of the lateral displacement of the reflected beam <sup>on the</sup> basis of the classical theory of diffraction. It is found that

$$D = - \frac{\lambda}{2\pi} \frac{d\phi}{di}$$

where  $D$  is the displacement

$\lambda$  is the wavelength in the denser medium

$\phi$  is the phase change at total reflection

and  $i$  is the angle of incidence.

REFERENCES

1. Artmann, K. Ann. Phys., Lpz. (F6) 2: 87. 1948.
2. Born, M. Optik. Julius Springer, Berlin. 1933. p. 41.
3. Bruhat, G. Cours D'Optique. Masson et Cie. Paris. 1931. p. 349.
4. Culshaw, W. and Jones, D. S. Proc. Phys. Soc., B, 66: 859. 1953
5. Gibellato, S. Nuovo Cim. 6: 344. 1949.
6. Goos, F. and Hanchen, H. Ann. Phys., Lpz. (F6) 1: 333. 1947.
7. Keys, J. E. M.Sc. Thesis, McMaster University, 1953
8. Montgomery, C. G. Editor. Technique of microwave measurements. McGraw-Hill Book Company, Inc., New York. 1947. p. 57.
9. Morgan, J. Introduction to Geometrical and Physical Optics. McGraw-Hill Book Company, Inc., New York. 1953. p. 205.
10. Row, R. V. J. Appl. Phys. 24: 1448. 1953.
11. Stratton, J. A. Electromagnetic Theory. McGraw-Hill Book Company, Inc., London. 1941. Sec. 9.7.
12. Wiles, S. T. M.Sc. Thesis, McMaster University, 1952.
13. Wood, R. W. Physical Optics, 2nd Edit. MacMillan Company, Toronto. 1911. p. 374.

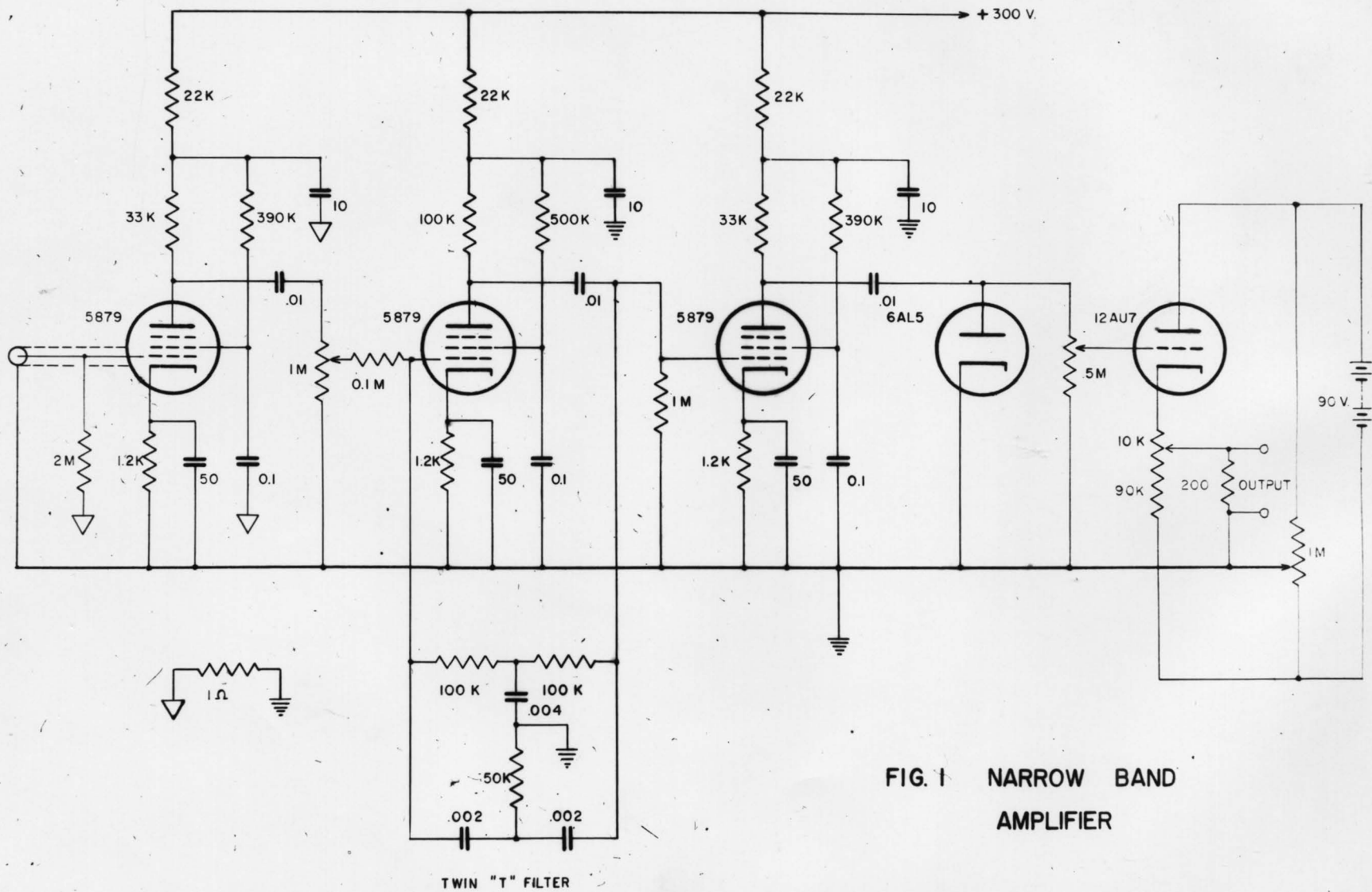


FIG. 1 NARROW BAND AMPLIFIER

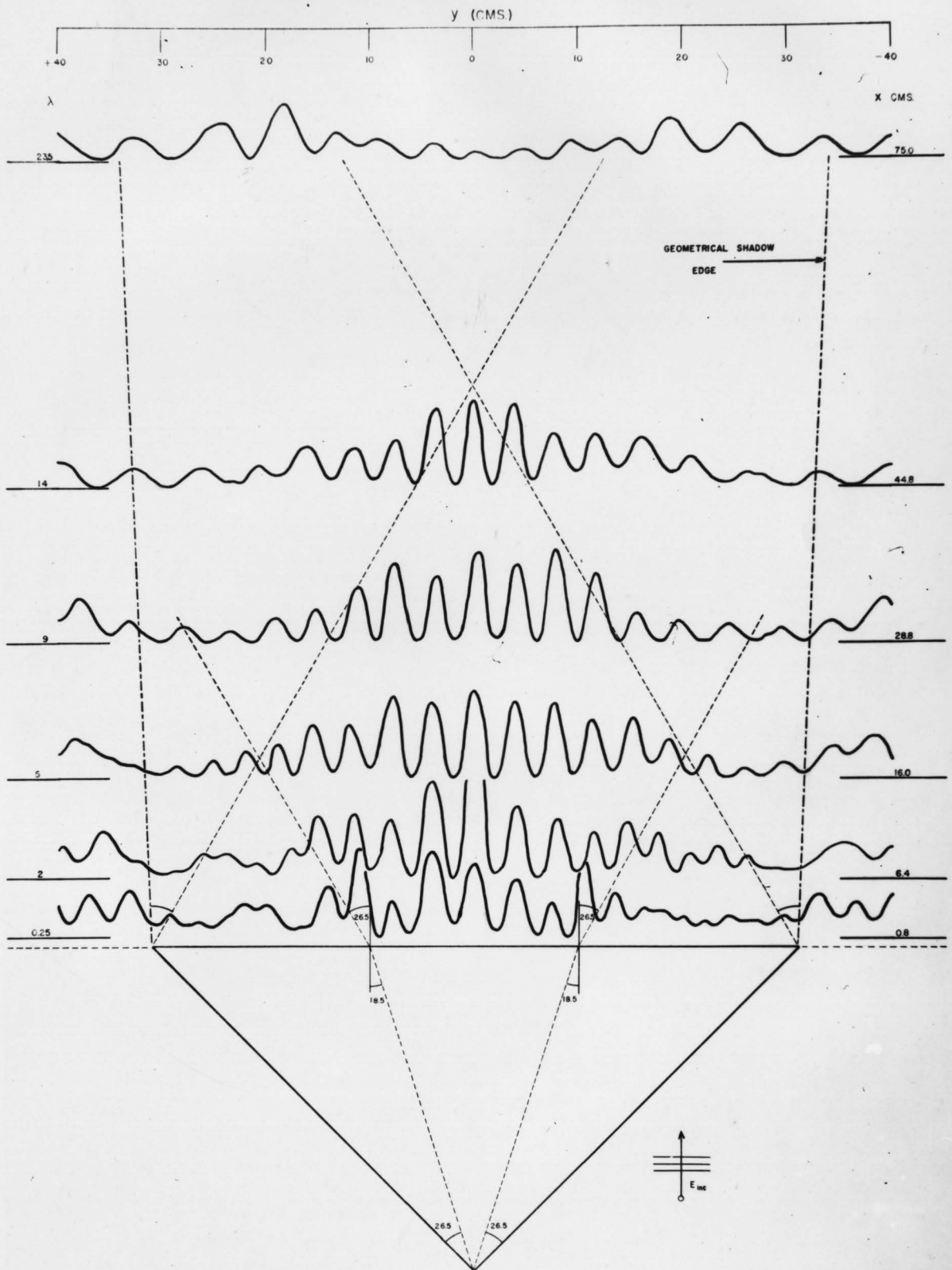


FIG. 2 EXPERIMENTAL INTERFERENCE AND DIFFRACTION FRINGES BEHIND THE BIPRISM

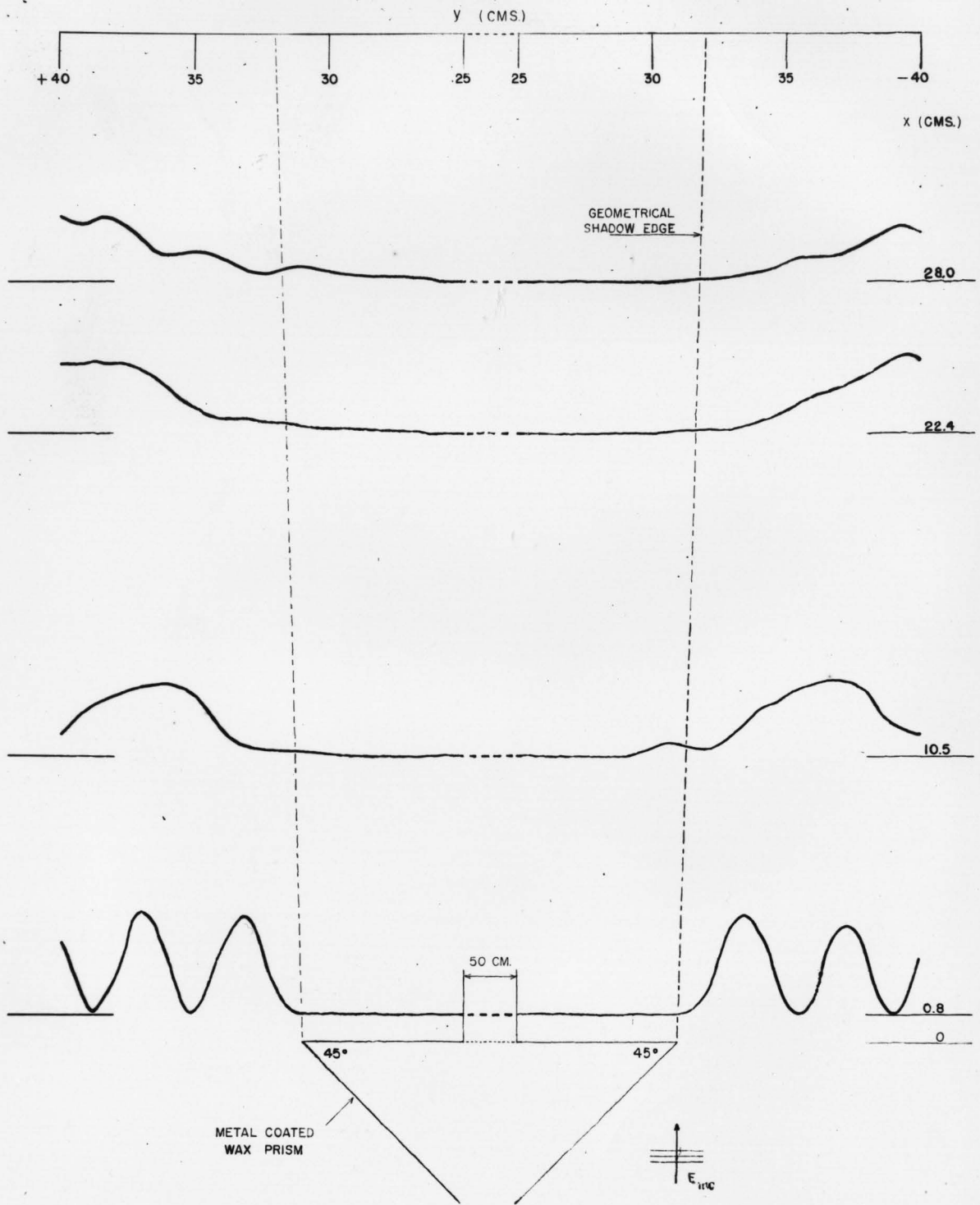


FIG. 3 DIFFRACTION FRINGES OF 45° CONDUCTING WEDGES

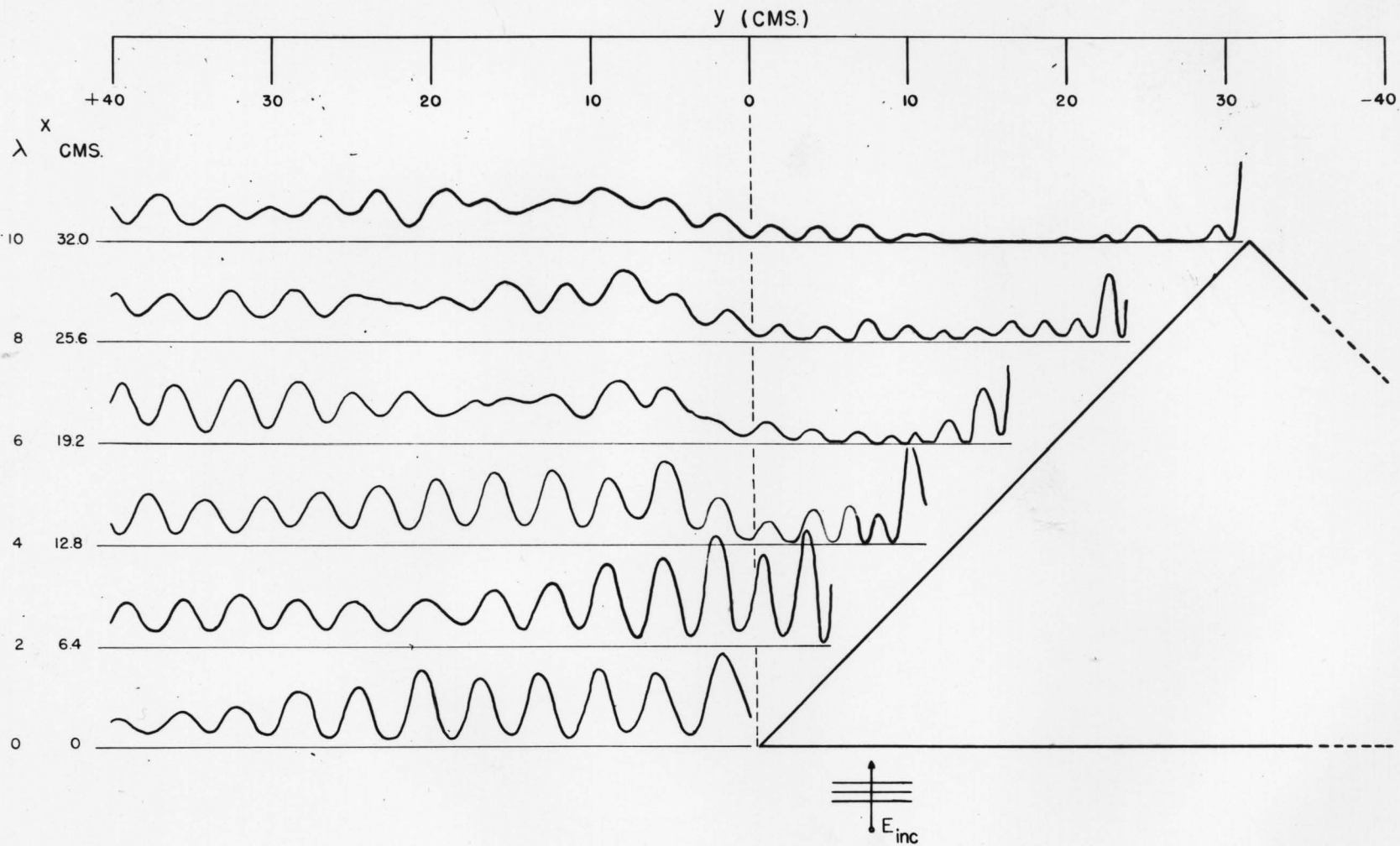


FIG. 4 DIFFRACTION FRINGES OF 45° DIELECTRIC WEDGE  
AND  
EVANESCENT WAVE AT A TOTALLY REFLECTING SURFACE

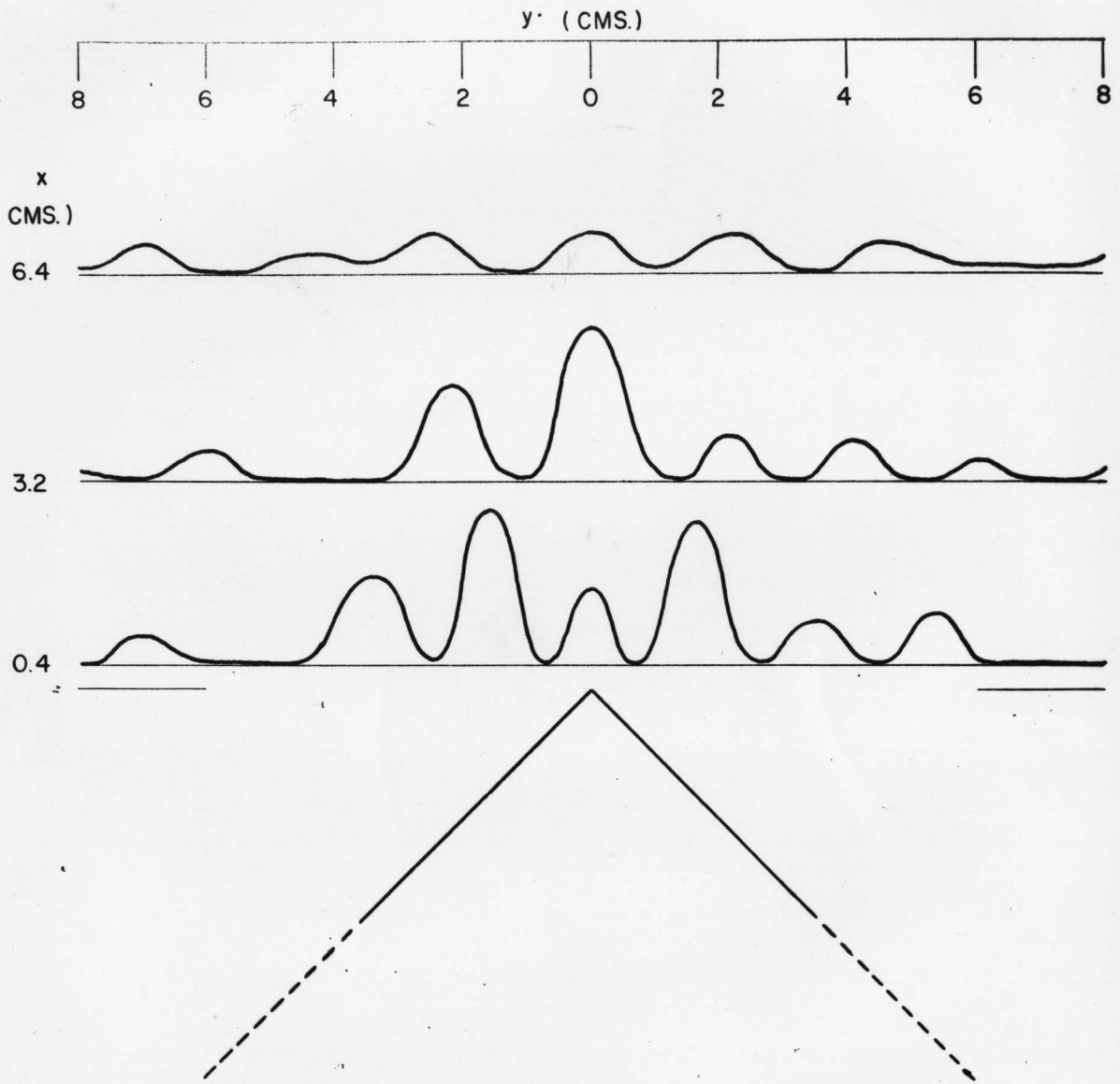


FIG. 5 INTERFERENCE FRINGES OF THE EVANESCENT WAVE BEHIND  
THE PRISM

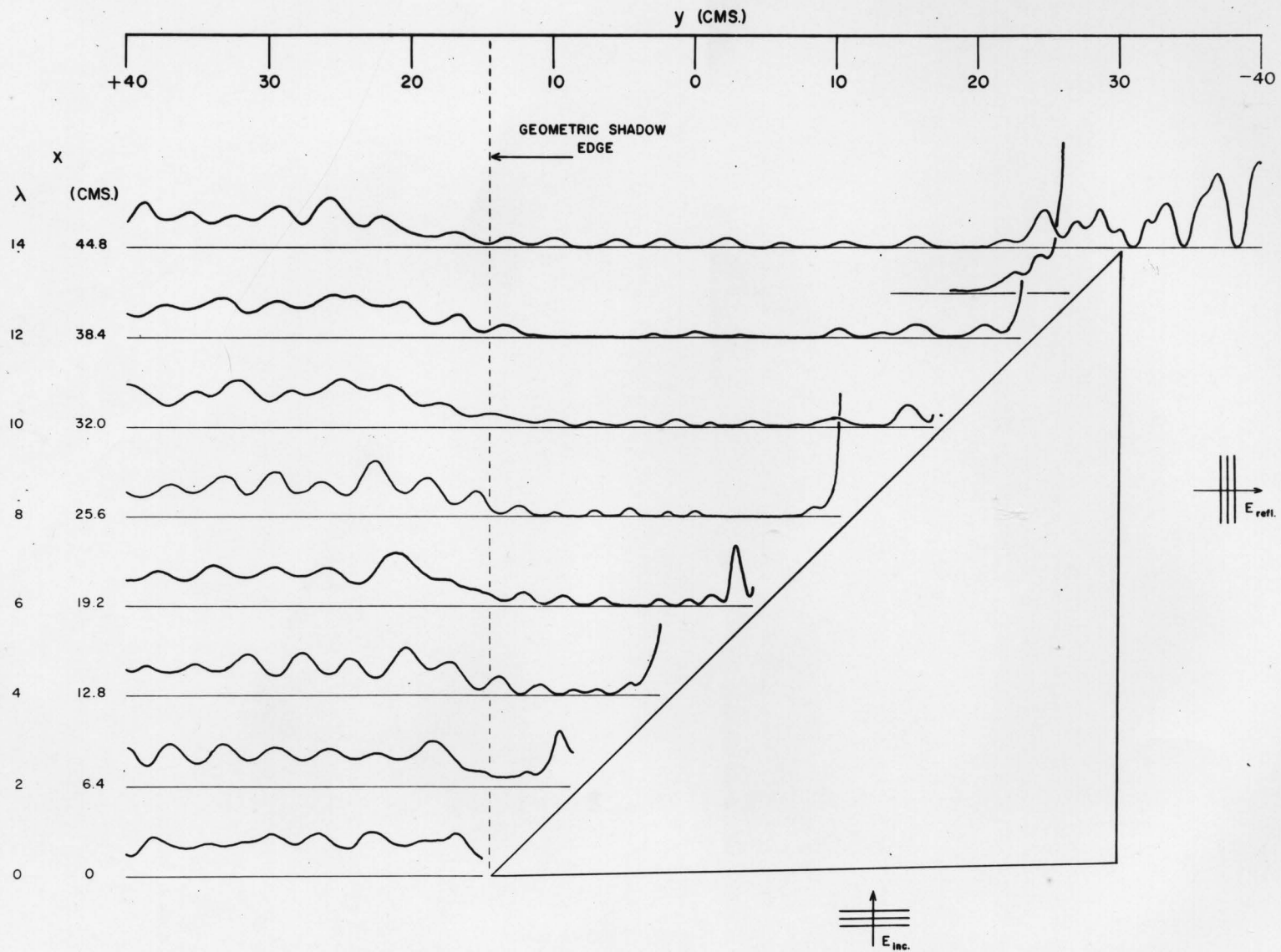


FIG. 6 THE FIELD BEHIND THE SINGLE REFLECTING PRISM 7



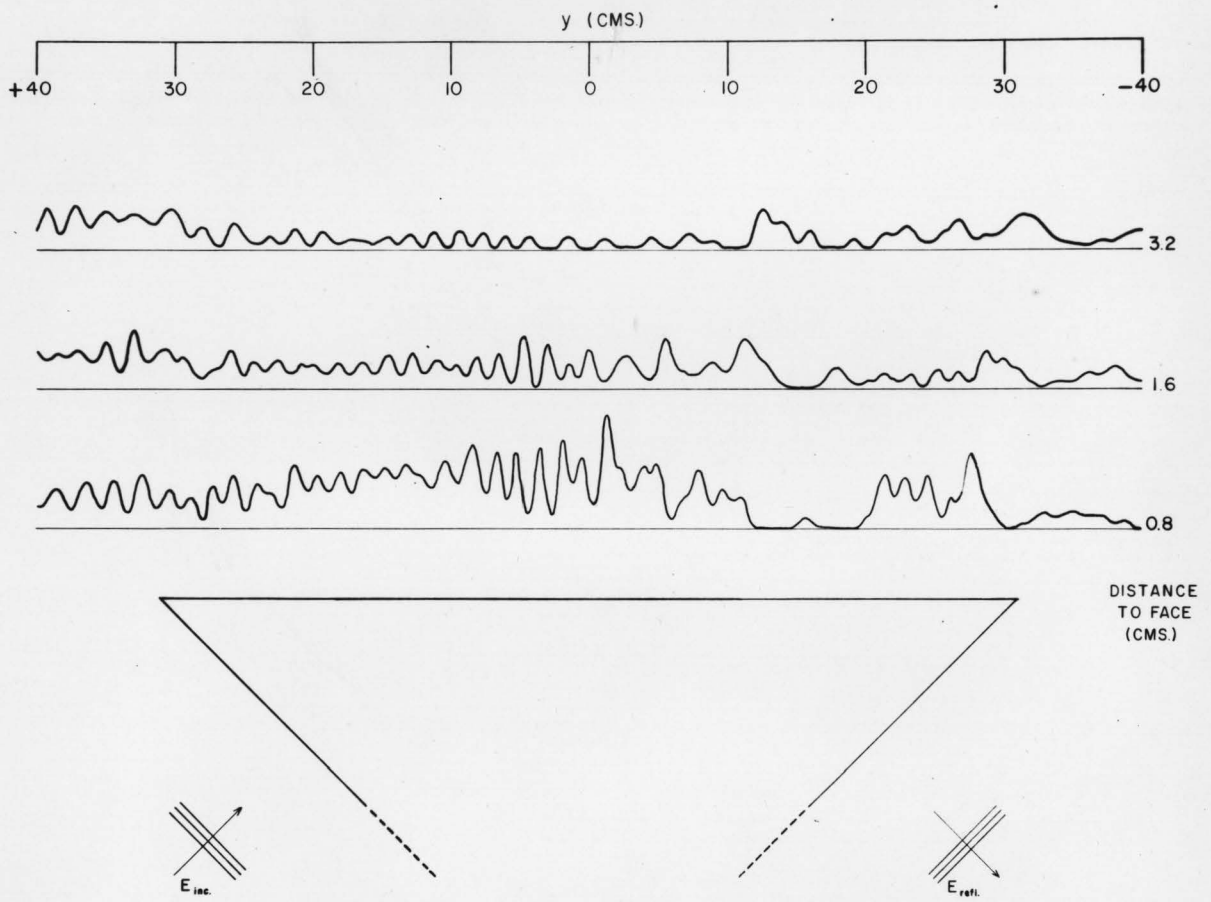


FIG. 7 EVANESCENT WAVE NEAR THE SURFACE OF THE TOTALLY REFLECTING PRISM